Quantum Inf Process (2016) 15:4729–4746
DOI 10.1007/s11128-016-1408-7

Two different types of optical hybrid qubits for teleportation in a lossy environment

Hoyong Kim[1] · **Seung-Woo Lee**[1,2] · **Hyunseok Jeong**[1]

Received: 3 March 2016 / Accepted: 21 July 2016 / Published online: 1 August 2016

Abstract We investigate the performance of quantum teleportation under a lossy environment using two different types of optical hybrid qubits. One is the hybrid of a polarized single-photon qubit and a coherent-state qubit (type-I logical qubit), and the other is the hybrid of a qubit of the vacuum and the single-photon and a coherent-state qubit (type-II logical qubit). We show that type-II hybrid qubits are generally more robust to photon loss effects compared to type-I hybrid qubits with respect to fidelities and success probabilities of quantum teleportation.

Keywords Quantum teleportation · Quantum information processing · Quantum optics · Optical qubit · Hybrid qubit · Decoherence

1 Introduction

Quantum teleportation is a protocol to transfer an unknown qubit from one place to another via an entangled quantum channel [1–3]. It is at the heart of various applications in quantum communication and computation. In particular, it plays a crucial role in implementing all-optical quantum computation [4–9]. A typical qubit for optical quantum teleportation utilizes the horizontal and vertical polarization states of a single photon, $\{|H\rangle, |V\rangle\}$ [2,5–7], or alternatively the vacuum and single-photon states, $\{|0\rangle, |1\rangle\}$ [10,11]. However, in this type of approaches based on a single-photon qubit, the success probability of a Bell-state measurement, which is an essential element in

✉ Hyunseok Jeong
h.jeong37@gmail.com

1 Department of Physics and Astronomy, Center for Macroscopic Quantum Control, Seoul National University, Seoul 08826, Korea

2 Quantum Universe Center, Korea Institute for Advanced Study, Seoul 02455, Korea

realizing the quantum teleportation protocol, cannot exceed 1/2 using linear optics and photon detection [12,13]. Efforts are being made to overcome this limitation using auxiliary states, additional operations or multipartite encoding [14–18], while each of them has its own price to pay. An alternative approach employs coherent states as the qubit basis, $\{|\alpha\rangle, |-\alpha\rangle\}$ [19,20], where $\pm\alpha$ are amplitudes of the coherent states. It enables one to implement a nearly deterministic Bell-state measurement [20–23]. However, due to the non-orthogonality of two coherent states, $|\alpha\rangle$ and $|-\alpha\rangle$, a necessary operation to finish the teleportation process such as the Pauli-Z operation cannot be performed in a deterministic way and produces additional errors [8,9].

Recently, a hybrid approach to optical quantum information processing was proposed by combining advantages of the two aforementioned approaches [24]. In this approach, the logical qubit is constructed using entanglement between the polarization states of a single photon and coherent states that leads to nearly deterministic quantum controls [24]. It enables one to perform a near-deterministic quantum teleportation as well as near-deterministic universal gate operations in a more efficient manner compared to previous approaches [4–9]. The required resource is hybrid states in the form of $|\mathrm{H_I}\rangle = |H\rangle|\alpha\rangle + |V\rangle|-\alpha\rangle$ [24]. Within this context, it was shown that such a hybrid entanglement is useful for teleportation between a polarized single-photon qubit and a coherent-state qubit [25] and for a loophole-free Bell inequality test [26]. However, it is known that the generation of entanglement between a polarized single photon and coherent states such as $|\mathrm{H_I}\rangle$ is highly demanding [27–30]. There exists a recent theoretical proposal that enables one to efficiently generate the state $|\mathrm{H_I}\rangle$ based on parametric downconversion, linear optics elements, and photodetectors [31], while it requires preparation of a coherent-state superposition [32] as a resource.

On the other hand, the hybrid entanglement of the vacuum and the single photon (instead of single-photon polarization) with coherent states, such as $|\mathrm{H_{II}}\rangle = |0\rangle|\alpha\rangle + |1\rangle|-\alpha\rangle$, was successfully demonstrated in recent experiments [33,34]. While $|\mathrm{H_{II}}\rangle$ is easier to generate than $|\mathrm{H_I}\rangle$, universal gate operations for a logical qubit in the form of $|\mathrm{H_{II}}\rangle$ are not so straightforward to implement. This is because single-qubit operations in the basis of the vacuum $|0\rangle$ and the single photon $|1\rangle$ except the phase rotation are basically non-deterministic [11]. Nevertheless, it was recently shown that the qubits utilizing the vacuum and the single photon basis are more robust against losses compared to the polarized single-photon qubits [35].

Thus, the two types of hybrid states $|\mathrm{H_I}\rangle$ and $|\mathrm{H_{II}}\rangle$ have their own advantages and disadvantages compared to each other for quantum information processing. However, we still do not have any clear references about the choice of the type in a specific scenario of the implementation of quantum information protocols. Therefore, it may be essential to investigate two distinct approaches under the same circumstances, one based on the form of $|\mathrm{H_I}\rangle$ and the other of $|\mathrm{H_{II}}\rangle$, and compare their performances regarding noises or resources for quantum information processing.

In this paper, we investigate the implementations of quantum teleportation in a lossy environment as a paradigmatic example to compare the two different types of hybrid qubits in the form of $|\mathrm{H_I}\rangle$ and $|\mathrm{H_{II}}\rangle$. We will consider the photon loss effect, which is the dominant noise factor for optical quantum information processing [9] among all possible decoherence effects during teleportation process [36–38]. We first analyze the effects of photon losses on the entangled quantum channel distributed between two separated parties, based on the two different hybrid states. We then compare their performances of quantum teleportation with respect to the average fidelity and the average success probability of teleportation. Our analysis shows that the quantum teleportation with the hybrid of a qubit of the vacuum and the single-photon and a coherent-state qubit $|\mathrm{H_{II}}\rangle$ is more robust to photon losses than the hybrid of a polarized single-photon qubit and a coherent-state qubit $|\mathrm{H_I}\rangle$.

2 Qunatum teleportation using hybrid qubits

2.1 Two types of optical hybrid qubits

Since there are a number of studies on quantum information processing using various kinds of optical hybrid systems [24,33,34,39–49], we first need to clarify the types of optical hybrid qubits that we consider in this paper. The first one is the hybrid of a polarized single-photon qubit and a coherent-state qubit, which was originally used to propose the hybrid scheme of optical quantum information processing recently [24]. The other is the hybrid of a qubit of the vacuum and the single-photon and a coherent-state qubit, which was recently generated by experiments [33,34]. We consider optical hybrid qubits constructed in the logical basis,

$$\{|0_L\rangle = |+\rangle|\alpha\rangle, |1_L\rangle = |-\rangle|-\alpha\rangle\}, \tag{1}$$

and the two different types of hybrid qubits are then defined as

I. the hybrid of a polarized single-photon qubit and a coherent-state qubit where $|\pm\rangle = (|H\rangle \pm |V\rangle)/\sqrt{2}$,
II. the hybrid of a qubit of the vacuum and the single-photon and a coherent-state qubit where $|\pm\rangle = (|0\rangle \pm |1\rangle)/\sqrt{2}$.

We will refer to the former as *type-I* hybrid qubit which is the same form used in Ref. [24], while the latter will be referred to as *type-II* hybrid qubit hereafter.

2.2 Teleportation scheme for hybrid qubits

In the standard quantum teleportation procedure [1], Alice is supposed to teleport an arbitrary unknown state $|\phi\rangle = \mu|0_L\rangle + \nu|1_L\rangle$ to Bob via a maximally entangled quantum channel $|\Psi_{ch}\rangle = (|0_L\rangle|0_L\rangle + |1_L\rangle|1_L\rangle)/\sqrt{2}$. Alice performs a Bell-state measurement on the unknown qubit and her part of the entangled channel and sends the measurement outcome to Bob. Bob applies an appropriate unitary transform on his state depending on Alice's measurement outcome in order to reconstruct the original qubit.

The hybrid teleportation scheme of type-I qubits is described in Ref. [24]. As shown in Fig. 1a, Alice and Bob share a hybrid entangled channel in order to teleport a type-I hybrid qubit from Alice to Bob. The total product state of the unknown input state $|\phi\rangle$ and the channel state $|\Psi_{ch}\rangle$ in terms of the type-I hybrid encoding can be expressed as

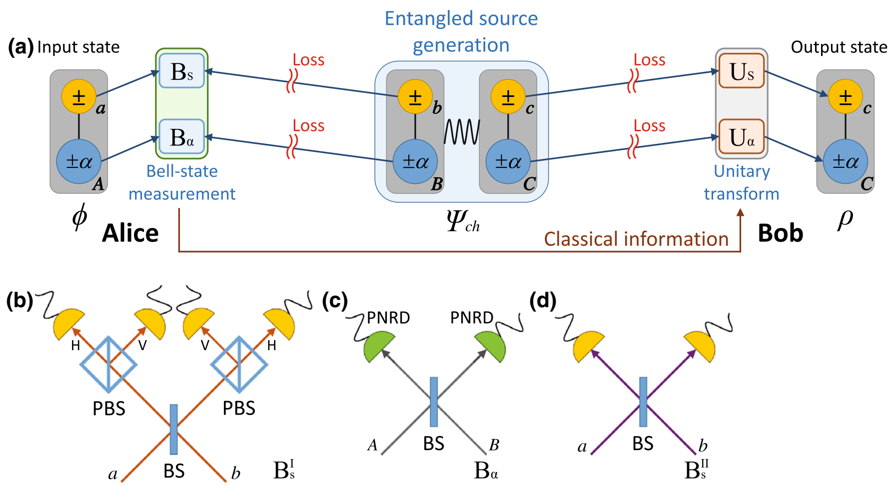

Fig. 1 (Color Online) **a** Schematic of hybrid quantum teleportation. Photon losses are supposed to occur in the channel state Ψ_{ch}. $\mathrm{U_s}$ (U_α) represents a unitary transform applied to a single-photon state (coherent state). ϕ and ρ represent the initial state and the final teleported state, respectively. The logical Bell-state measurement is composed of two elements, $\mathrm{B_s}$ and B_α, that correspond to Bell-state measurements for single-photon states and coherent states, respectively. **b** When type-I hybrid qubits are used, $\mathrm{B_s^I}$ is performed using a 50:50 beam splitter (BS), two polarizing beam splitters (PBS) and four single-photon detectors [12]. **c** B_α is implemented using a 50:50 beam splitter and two photon-number-resolving detectors (PNRD) [20]. **d** In the case of type-II hybrid qubits, $\mathrm{B_s^{II}}$ is implemented using a 50:50 beam splitter and two single-photon detectors [10]

$$|\phi\rangle_{aA}|\Psi_{ch}\rangle_{bBcC} = \frac{1}{2}\Big(|\Phi_L^+\rangle_{aAbB}|\phi\rangle_{cC} + |\Phi_L^-\rangle_{aAbB}\hat{Z}|\phi\rangle_{cC} + |\Psi_L^+\rangle_{aAbB}\hat{X}|\phi\rangle_{cC} + |\Psi_L^-\rangle_{aAbB}\hat{X}\hat{Z}|\phi\rangle_{cC}\Big), \tag{2}$$

with logical Bell states

$$|\Phi_L^\pm\rangle = \frac{1}{\sqrt{2}}(|0_L\rangle|0_L\rangle \pm |1_L\rangle|1_L\rangle), \tag{3}$$

$$|\Psi_L^\pm\rangle = \frac{1}{\sqrt{2}}(|0_L\rangle|1_L\rangle \pm |1_L\rangle|0_L\rangle), \tag{4}$$

and Pauli operators $\hat{X}$ and $\hat{Z}$ in terms of the logical qubit basis, where subscripts a, b and c in Eq. (2) represent single-photon modes and A, B and C represent coherent-state modes as depicted in Fig. 1a. This equation can be rewritten as

$$|\phi\rangle_{aA}|\Psi_{ch}\rangle_{bBcC} = \frac{1}{4}\Bigg[\left(\frac{|\Phi_{\mathrm{I}}^+\rangle_{ab}|\Phi_\alpha^+\rangle_{AB}}{N_\alpha^+} + \frac{|\Psi_{\mathrm{I}}^+\rangle_{ab}|\Phi_\alpha^-\rangle_{AB}}{N_\alpha^-}\right)|\phi\rangle_{cC} + \left(\frac{|\Phi_{\mathrm{I}}^+\rangle_{ab}|\Phi_\alpha^-\rangle_{AB}}{N_\alpha^-} + \frac{|\Psi_{\mathrm{I}}^+\rangle_{ab}|\Phi_\alpha^+\rangle_{AB}}{N_\alpha^+}\right)\hat{Z}|\phi\rangle_{cC}$$

$$+\left(\frac{|\Phi_{\mathrm{I}}^{-}\rangle_{ab}|\Psi_{\alpha}^{+}\rangle_{AB}}{N_{\alpha}^{+}}-\frac{|\Psi_{\mathrm{I}}^{-}\rangle_{ab}|\Psi_{\alpha}^{-}\rangle_{AB}}{N_{\alpha}^{-}}\right)\hat{X}|\phi\rangle_{cC}$$
$$+\left(\frac{|\Phi_{\mathrm{I}}^{-}\rangle_{ab}|\Psi_{\alpha}^{-}\rangle_{AB}}{N_{\alpha}^{-}}-\frac{|\Psi_{\mathrm{I}}^{-}\rangle_{ab}|\Psi_{\alpha}^{+}\rangle_{AB}}{N_{\alpha}^{+}}\right)\hat{X}\hat{Z}|\phi\rangle_{cC}\Bigg], \quad (5)$$

where

$$|\Phi_{\mathrm{I}}^{\pm}\rangle=\frac{1}{\sqrt{2}}(|H\rangle|H\rangle\pm|V\rangle|V\rangle), \quad (6)$$
$$|\Psi_{\mathrm{I}}^{\pm}\rangle=\frac{1}{\sqrt{2}}(|H\rangle|V\rangle\pm|V\rangle|H\rangle), \quad (7)$$

and

$$|\Phi_{\alpha}^{\pm}\rangle=N_{\alpha}^{\pm}(|\alpha\rangle|\alpha\rangle\pm|-\alpha\rangle|-\alpha\rangle), \quad (8)$$
$$|\Psi_{\alpha}^{\pm}\rangle=N_{\alpha}^{\pm}(|\alpha\rangle|-\alpha\rangle\pm|-\alpha\rangle|\alpha\rangle), \quad (9)$$

with $N_{\alpha}^{\pm}=1/\sqrt{2\pm 2e^{-4|\alpha|^2}}$. Comparing Eqs. (2) and (5), we notice that in order to perform the logical Bell-state measurement to discriminate between four logical Bell states in Eqs. (3) and (4), one needs to perform two small Bell measurement units, i.e., one for $|\Phi_{\mathrm{I}}^{\pm}\rangle$ and $|\Psi_{\mathrm{I}}^{\pm}\rangle$ and the other is for $|\Phi_{\alpha}^{\pm}\rangle$ and $|\Psi_{\alpha}^{\pm}\rangle$ as shown in Eq. (5). Thus, the Bell-state measurement for the polarized single-photon states ($\mathrm{B}_{\mathrm{s}}^{\mathrm{I}}$ for modes a and b) and another Bell-state measurement for the coherent states (B_{α} for modes A and B) should be performed as illustrated in Fig. 1a. For example, if $|\Phi_{\mathrm{I}}^{+}\rangle$ is detected by $\mathrm{B}_{\mathrm{s}}^{\mathrm{I}}$ and $|\Phi_{\alpha}^{+}\rangle$ is detected by B_{α}, one can conclude that one of the logical Bell states, $|\Phi_{L}^{+}\rangle$, has been measured.

The $\mathrm{B}_{\mathrm{s}}^{\mathrm{I}}$ measurement can be taken using a 50:50 beam splitter, two polarizing beam splitters and four single-photon detectors as shown in Fig. 1b [12]. Here, the single-photon detectors should be able to discriminate between zero, one and more than one photons. We define the 50:50 beam splitter operator as

$$U_{i,j}=e^{-\frac{\pi}{4}(a_i^{\dagger}a_j-a_ia_j^{\dagger})}, \quad (10)$$

where i and j are two field modes entering the beam splitter and a_i ($a_i^{\dagger}$) is the annihilation (creation) operator for mode i. After the action of the beam splitter $U_{a,b}$ which is applied to single-photon qubits of modes a and b, the output states of the Bell states of polarized single-photon states are

$$|\Psi_{\mathrm{I}}^{+}\rangle \xrightarrow{BS} \frac{1}{\sqrt{2}}(|HV\rangle|0\rangle-|0\rangle|HV\rangle), \quad (11)$$
$$|\Psi_{\mathrm{I}}^{-}\rangle \xrightarrow{BS} \frac{1}{\sqrt{2}}(|H\rangle|V\rangle-|V\rangle|H\rangle), \quad (12)$$
$$|\Phi_{\mathrm{I}}^{\pm}\rangle \xrightarrow{BS} \frac{1}{2}(|HH\rangle|0\rangle-|0\rangle|HH\rangle)\pm\frac{1}{2}(|VV\rangle|0\rangle-|0\rangle|VV\rangle). \quad (13)$$

By detecting one photon at one detector and one photon at another detector, two ($|\Psi_{\mathrm{I}}^{+}\rangle$ and $|\Psi_{\mathrm{I}}^{-}\rangle$) of the four Bell states can be discriminated. If two photons are detected at one detector, we cannot figure out whether it was $|\Phi_{\mathrm{I}}^{+}\rangle$ or $|\Phi_{\mathrm{I}}^{-}\rangle$ which means a measurement failure.

The B_α measurement is implemented in a nearly deterministic way using a 50:50 beam splitter and two photon-number-resolving detectors as shown in Fig. 1c [20]. The operation of the beam splitter $U_{A,B}$ on coherent states is characterized as $U_{A,B}|\alpha\rangle_A|\beta\rangle_B = |(\alpha+\beta)/\sqrt{2}\rangle_A|(-\alpha+\beta)/\sqrt{2}\rangle_B$. The Bell states of coherent states after passing through the beam splitter $U_{A,B}$ are

$$|\Phi_\alpha^{\pm}\rangle_{AB} \xrightarrow{BS} N_\alpha^{\pm}(|\sqrt{2}\alpha\rangle \pm |-\sqrt{2}\alpha\rangle)_A|0\rangle_B, \tag{14}$$

$$|\Psi_\alpha^{\pm}\rangle_{AB} \xrightarrow{BS} N_\alpha^{\pm}|0\rangle_A(|\sqrt{2}\alpha\rangle \pm |-\sqrt{2}\alpha\rangle)_B, \tag{15}$$

where $|\mathrm{even}\rangle \equiv N_\alpha^{+}(|\sqrt{2}\alpha\rangle + |-\sqrt{2}\alpha\rangle)$ and $|\mathrm{odd}\rangle \equiv N_\alpha^{-}(|\sqrt{2}\alpha\rangle - |-\sqrt{2}\alpha\rangle)$ are even and odd number states which contain only even and odd number of photons, respectively. The four Bell states of coherent states can be discriminated using two photon-number-resolving measurements as

$$\begin{aligned}&(\mathrm{even}, 0) : \Phi_\alpha^{+}, \quad (\mathrm{odd}, 0) : \Phi_\alpha^{-},\\ &(0, \mathrm{even}) : \Psi_\alpha^{+}, \quad (0, \mathrm{odd}) : \Psi_\alpha^{-}.\end{aligned} \tag{16}$$

If even number of photons are detected at mode A and no photon is detected at mode B, it means that the Bell state was $|\Phi_\alpha^{+}\rangle$, and so on. The failure of B_α occurs when both the detectors are silent due to the vacuum portion in state $|\mathrm{even}\rangle$.

If we assume that available resources are linear optics elements and photodetectors (either single-photon detectors or number-resolving detectors), the success probability of $\mathrm{B}_{\mathrm{s}}^{\mathrm{I}}$ is limited to 1/2 [12,13] and the success probability of the B_α is $1-\exp(-2|\alpha|^2)$ [24]. A remarkable advantage of the scheme based on the hybrid qubits is that the whole teleportation process can be made successful as far as one of the two measurement elements, $\mathrm{B}_{\mathrm{s}}^{\mathrm{I}}$ or B_α, succeeds. To see this, consider the case of the measurement failure of $\mathrm{B}_{\mathrm{s}}^{\mathrm{I}}$, which means that one cannot figure out whether the state was $|\Phi_{\mathrm{I}}^{+}\rangle$ or $|\Phi_{\mathrm{I}}^{-}\rangle$. The possible measurement outcomes according to the measurement result of B_α are then $|\Phi_{\mathrm{I}}^{+}\rangle|\Phi_\alpha^{+}\rangle$, $|\Phi_{\mathrm{I}}^{+}\rangle|\Phi_\alpha^{-}\rangle$, $|\Phi_{\mathrm{I}}^{-}\rangle|\Psi_\alpha^{+}\rangle$, or $|\Phi_{\mathrm{I}}^{-}\rangle|\Psi_\alpha^{-}\rangle$ as shown in Eq. (5). Thus, the success of the B_α measurement results in the success of the whole teleportation process. In the case of the measurement failure of B_α, in which one cannot figure out whether it was $|\Phi_\alpha^{+}\rangle$ or $|\Psi_\alpha^{+}\rangle$, the possible measurement outcomes according to the measurement result of $\mathrm{B}_{\mathrm{s}}^{\mathrm{I}}$ are $|\Phi_{\mathrm{I}}^{+}\rangle|\Phi_\alpha^{+}\rangle$, $|\Psi_{\mathrm{I}}^{+}\rangle|\Phi_\alpha^{+}\rangle$, $|\Phi_{\mathrm{I}}^{-}\rangle|\Psi_\alpha^{+}\rangle$, or $|\Psi_{\mathrm{I}}^{-}\rangle|\Psi_\alpha^{+}\rangle$ as shown in Eq. (5). Thus, the success of the $\mathrm{B}_{\mathrm{s}}^{\mathrm{I}}$ measurement results in the success of the whole teleportation process too. In this way, the success probability of teleportation of a hybrid qubit is $P_h = 1-\exp(-2|\alpha|^2)/2$ [24].

To complete the teleportation process, an appropriate Pauli operation ($\mathbb{1}$, $\hat{Z}$, $\hat{X}$, or $\hat{X}\hat{Z}$) should be applied according to the measurement result (U_{s} and U_α in Fig. 1a). The Pauli operations for type-I hybrid qubits in the logical basis (1) can be done deterministically [24]. The Pauli X operation can be performed by applying a bit flip operation on each of the two modes. The implementations of a polarization rotator on the polarized single-photon states ($|+\rangle \leftrightarrow |-\rangle$), where $|\pm\rangle = (|H\rangle \pm |V\rangle)/\sqrt{2}$, and a π phase shifter on the coherent states ($|\alpha\rangle \leftrightarrow |-\alpha\rangle$) accomplish the Pauli X operation. The Pauli Z operation is performed by applying the π phase shift operation on the polarized single-photon states ($|\pm\rangle \rightarrow \pm|\pm\rangle$), and no operation is required on the coherent states.

The hybrid teleportation of type-II qubits can be carried out similarly to the case of type-I. The total product state of an unknown input state $|\phi\rangle$ and the channel state $|\Psi_{ch}\rangle$ can be written as Eq. (5) by replacing $|\Phi_{\rm I}^{\pm}\rangle$ and $|\Psi_{\rm I}^{\pm}\rangle$ with the Bell states of the vacuum and the single-photon states $|\Phi_{\rm II}^{\pm}\rangle$ and $|\Psi_{\rm II}^{\pm}\rangle$, respectively, which are defind as

$$|\Phi_{\rm II}^{\pm}\rangle = (|0\rangle|0\rangle \pm |1\rangle|1\rangle)/\sqrt{2}, \tag{17}$$

$$|\Psi_{\rm II}^{\pm}\rangle = (|0\rangle|1\rangle \pm |1\rangle|0\rangle)/\sqrt{2}. \tag{18}$$

The Bell-state measurement for the vacuum and the single-photon states, $\mathrm{B}_{\mathrm{s}}^{\mathrm{II}}$, and the Bell-state measurement for the coherent states, B_{α}, should then be performed. The $\mathrm{B}_{\mathrm{s}}^{\mathrm{II}}$ measurement can be performed using a 50:50 beam splitter and two single-photon detectors as shown in Fig. 1d with the success probability of 1/2 [10]. By applying the beam splitter operation $U_{a,b}$, the Bell states of the vacuum and the single-photon states are transformed as

$$|\Psi_{\rm II}^{+}\rangle \xrightarrow{BS} |0\rangle|1\rangle, \tag{19}$$

$$|\Psi_{\rm II}^{-}\rangle \xrightarrow{BS} |1\rangle|0\rangle, \tag{20}$$

$$|\Phi_{\rm II}^{\pm}\rangle \xrightarrow{BS} \frac{1}{2}(|0\rangle|2\rangle - |2\rangle|0\rangle) \pm \frac{1}{\sqrt{2}}|0\rangle|0\rangle. \tag{21}$$

If one photon is detected at one detector and the other detector is silent, one can identify whether it was $|\Psi_{\rm II}^{+}\rangle$ or $|\Psi_{\rm II}^{-}\rangle$. However, if two photons are detected at one detector or both detectors are silent, we cannot find whether it was $|\Phi_{\rm II}^{+}\rangle$ or $|\Phi_{\rm II}^{-}\rangle$.

The Pauli X operation for type-II hybrid qubits in the logical basis (1) can be implemented by acting the π phase shift on each of the two modes. However, the Pauli Z operation for type-II hybrid qubits cannot be performed deterministically. In order to perform the Pauli Z operation for type-II hybrid qubits, one needs a bit flip between $|0\rangle$ and $|1\rangle$ (i.e., $|0\rangle \leftrightarrow |1\rangle$) for the vacuum and the single-photon states or a sign flip for the coherent states ($|\pm\alpha\rangle \rightarrow \pm|\pm\alpha\rangle$) which can be implemented non-deterministically [8,11]. One simple working solution is to "logically relabel" the vacuum and the single photon, $|0\rangle$ and $|1\rangle$, whenever it is necessary. In other words, we know that $|0\rangle$ and $|1\rangle$ remain unaltered, whenever they should be altered, so that it can be logically corrected at the final measurement stage. Under the assumption above, the success probability of quantum teleportation for type-II hybrid qubits is the same to that for type-I qubits $P_h = 1 - \exp(-2|\alpha|^2)/2$.

2.3 Generation scheme for the channel state of type-II hybrid qubits

The channel state $|\Psi_{ch}\rangle$ for the quantum teleportation of the type-I hybrid qubits can be generated using two hybrid pairs, $|H\rangle|\sqrt{2}\alpha\rangle + |V\rangle|-\sqrt{2}\alpha\rangle$ [24]. Similarly, one can generate the channel state of the type-II hybrid qubits using two resource states $|+\rangle|\sqrt{2}\alpha\rangle + |-\rangle|-\sqrt{2}\alpha\rangle$, where $|\pm\rangle = (|0\rangle \pm |1\rangle)/\sqrt{2}$, which was experimentally demonstrated recently [34] and the Bell-state measurement of the coherent states, B_α. The resource states can be transformed to $|+\rangle|\alpha\rangle|-\alpha\rangle + |-\rangle|-\alpha\rangle|\alpha\rangle = |0_L\rangle|-\alpha\rangle + |1_L\rangle|\alpha\rangle$ by applying the 50:50 beam splitter on the coherent states. To perform the B_α measurement on these states, one of the coherent states of each state are mixed by a 50:50 beam splitter, such that the total state evolves as

$$\begin{aligned}
&(|0_L\rangle|-\alpha\rangle + |1_L\rangle|\alpha\rangle)(|0_L\rangle|-\alpha\rangle + |1_L\rangle|\alpha\rangle)\\
&\xrightarrow{BS} (|0_L\rangle|0_L\rangle + |1_L\rangle|1_L\rangle)\frac{1}{2N_\alpha^+}|\mathrm{even}\rangle|0\rangle - (|0_L\rangle|0_L\rangle - |1_L\rangle|1_L\rangle)\frac{1}{2N_\alpha^-}|\mathrm{odd}\rangle|0\rangle\\
&\quad + (|0_L\rangle|1_L\rangle + |1_L\rangle|0_L\rangle)\frac{1}{2N_\alpha^+}|0\rangle|\mathrm{even}\rangle + (|0_L\rangle|1_L\rangle - |1_L\rangle|0_L\rangle)\frac{1}{2N_\alpha^-}|0\rangle|\mathrm{odd}\rangle.
\end{aligned} \tag{22}$$

After the measurement of two photon-number-resolving detectors, the possible obtained states are $|0_L\rangle|0_L\rangle \pm |1_L\rangle|1_L\rangle$ and $|0_L\rangle|1_L\rangle \pm |1_L\rangle|0_L\rangle$. The latter states can be transformed to the former by applying the Pauli X operation on one of the logical qubits. Therefore, the channel state $|0_L\rangle|0_L\rangle + |1_L\rangle|1_L\rangle$ is generated with success probability $[1-\exp(-2|\alpha|^2)]^2/2$. We note that the state $|0_L\rangle|0_L\rangle - |1_L\rangle|1_L\rangle$ can also be used as a channel state. The only change caused by using the channel state $|0_L\rangle|0_L\rangle - |1_L\rangle|1_L\rangle$ instead of $|0_L\rangle|0_L\rangle + |1_L\rangle|1_L\rangle$ for the quantum teleportation is that the appropriate unitary transformations which are required in the last step of the teleportation process are switched by the amount of the Pauli Z operation ($\mathbb{1} \leftrightarrow \hat{Z}$, $\hat{X} \leftrightarrow \hat{X}\hat{Z}$).

3 Quantum teleportation for hybrid qubits under photon losses

In an ideal situation, quantum teleportation can be carried out with the unit success probability and the teleported state should be exactly the same to the input state. However, in realistic implementations, there are factors that reduce the success probability and the teleportation fidelity. Here, we consider two major such factors. One is inefficiency of the Bell-state measurement, and the other is photon losses in the quantum channel as shown in Fig. 1a. In the following subsections, we will calculate and compare the fidelities between the input and the output states and the success probabilities of teleportation for two different types of hybrid qubits.

3.1 Teleportation of type-I hybrid qubits

The time evolution of density operator ρ under photon losses is governed by the Born-Markov master equation [50],

$$\frac{\partial\rho}{\partial\tau} = \hat{J}\rho + \hat{L}\rho, \tag{23}$$

where τ is the interaction time, $\hat{J}\rho = \gamma \Sigma_i a_i \rho a_i^\dagger$, $\hat{L}\rho = -(\gamma/2)\Sigma_i (a_i^\dagger a_i \rho + \rho a_i^\dagger a_i)$, and γ is the decay constant. The general solution of Eq. (23) is written as, $\rho(\tau) = \exp[(\hat{J} + \hat{L})\tau]\rho(0)$, where $\rho(0)$ is the initial density operator [51]. We assume that each mode of the channel state $|\Psi_{ch}\rangle$ suffers the same decoherence rate characterized by γ. The entangled channel of the type-I hybrid qubits at time τ under the above assumption is obtained using Eq. (23) as

$$\begin{aligned}\rho_{\mathrm{I}}^{ch}(\tau) = \frac{1}{2}\Big\{&\big[\big(t^2|+\rangle\langle+| + r^2|0\rangle\langle 0|\big) \otimes |t\alpha\rangle\langle t\alpha|\big]^{\otimes 2} \\ &+ \big[\big(t^2|-\rangle\langle-| + r^2|0\rangle\langle 0|\big) \otimes |-t\alpha\rangle\langle -t\alpha|\big]^{\otimes 2} \\ &+ \big[t^2 e^{-2|\alpha|^2 r^2}|+\rangle\langle-| \otimes |t\alpha\rangle\langle -t\alpha|\big]^{\otimes 2} \\ &+ \big[t^2 e^{-2|\alpha|^2 r^2}|-\rangle\langle+| \otimes |-t\alpha\rangle\langle t\alpha|\big]^{\otimes 2}\Big\},\end{aligned} \tag{24}$$

where $|\pm\rangle = (|H\rangle \pm |V\rangle)/\sqrt{2}$, $t = e^{-\gamma\tau/2}$, $r = \sqrt{1 - e^{-\gamma\tau}}$, and $[\cdot]^{\otimes 2}$ means the direct product of same states. The parameter r containing both the real time τ and the decoherence rate γ will be used as the normalized time. As we see in Eq. (24), coherent-state qubits not only lose their relative phase information but also undergo amplitude damping by photon losses. However, we know the value of the interaction time τ, and we can use $|\pm t\alpha\rangle$ as a dynamic qubit basis in order to reflect the amplitude damping as suggested in Ref. [20]. The Bell states of coherent states using the dynamic qubit basis can be defined as

$$|\Phi_\alpha^\pm(\tau)\rangle = N_\alpha^\pm(\tau)(|t\alpha\rangle|t\alpha\rangle \pm |-t\alpha\rangle|-t\alpha\rangle), \tag{25}$$

$$|\Psi_\alpha^\pm(\tau)\rangle = N_\alpha^\pm(\tau)(|t\alpha\rangle|-t\alpha\rangle \pm |-t\alpha\rangle|t\alpha\rangle), \tag{26}$$

where $N_\alpha^\pm(\tau) = 1/\sqrt{2 \pm 2e^{-4t^2|\alpha|^2}}$. Adopting this, we define a dynamic orthonormal basis of optical hybrid qubits as

$$\{|0_L(\tau)\rangle = |+\rangle|t\alpha\rangle, |1_L(\tau)\rangle = |-\rangle|-t\alpha\rangle\}, \tag{27}$$

where $|\pm\rangle = (|H\rangle \pm |V\rangle)/\sqrt{2}$ and an unknown hybrid qubit which Alice wants to teleport as $|\phi(\tau)\rangle = \mu|0_L(\tau)\rangle + \nu|1_L(\tau)\rangle$ where $\mu = \cos(u/2)$ and $\nu = e^{iv}\sin(u/2)$. The logical Bell-state measurement should then be taken on the input state $|\phi(\tau)\rangle$ and one part of the decohered channel state $\rho_{\mathrm{I}}^{ch}(\tau)$. The Bell-state measurement for the polarized single-photon states, $\mathrm{B}_{\mathrm{s}}^{\mathrm{I}}$, and that of the coherent states, B_α, are taken [24]. The B_α measurement is represented by the projection operators:

$$O_1 = \sum_{n=1}^{\infty} |2n\rangle_A\langle 2n| \otimes |0\rangle_B\langle 0|, \tag{28}$$

$$O_2 = \sum_{n=1}^{\infty} |2n-1\rangle_A\langle 2n-1| \otimes |0\rangle_B\langle 0|, \tag{29}$$

$$O_3 = \sum_{n=1}^{\infty} |0\rangle_A\langle 0| \otimes |2n\rangle_B\langle 2n|, \tag{30}$$

$$O_4 = \sum_{n=1}^{\infty} |0\rangle_A\langle 0| \otimes |2n-1\rangle_B\langle 2n-1|, \tag{31}$$

$$O_{\mathrm{e}} = |0\rangle_A\langle 0| \otimes |0\rangle_B\langle 0|, \tag{32}$$

where subscripts 1, 2, 3 and 4 correspond to Φ_α^+, Φ_α^-, Ψ_α^+ and Ψ_α^-, respectively, while O_{e} represents the measurement failure for which both the detectors do not register any photon. The $\mathrm{B_s^I}$ measurement is represented by following projection operators,

$$M_1 = |HV\rangle_a\langle HV| \otimes |0\rangle_b\langle 0| + |0\rangle_a\langle 0| \otimes |HV\rangle_b\langle HV|, \tag{33}$$

$$M_2 = |H\rangle_a\langle H| \otimes |V\rangle_b\langle V| + |V\rangle_a\langle V| \otimes |H\rangle_b\langle H|, \tag{34}$$

$$\begin{aligned} M_{\mathrm{e}} = &|HH\rangle_a\langle HH| \otimes |0\rangle_b\langle 0| + |0\rangle_a\langle 0| \otimes |HH\rangle_b\langle HH| \\ &+ |VV\rangle_a\langle VV| \otimes |0\rangle_b\langle 0| + |0\rangle_a\langle 0| \otimes |VV\rangle_b\langle VV|, \end{aligned} \tag{35}$$

where M_1 and M_2 correspond to Ψ_{I}^+ and Ψ_{I}^-, respectively, while M_{e} represents a measurement failure. The teleportation process will be successful unless both B_α and $\mathrm{B_s^I}$ fail.

The unnormalized output state after measurement outcome $M_i \otimes O_j$ is obtained as

$$\rho^{i,j} = \mathrm{Tr}_{a,b,A,B}[(U_{a,b} \otimes U_{A,B})(|\phi(\tau)\rangle\langle\phi(\tau)| \otimes \rho_{\mathrm{I}}^{ch}(\tau))(U_{a,b}^\dagger \otimes U_{A,B}^\dagger)(M_i \otimes O_j)], \tag{36}$$

where the partial trace is taken over Alice's modes a, b, A and B in Fig. 1a. Finally, Bob should perform appropriate unitary operations ($\mathbb{1}$, $\hat{Z}$, $\hat{X}$, or $\hat{X}\hat{Z}$) according to Alice's measurement results. The details are as follows: $\mathbb{1}$ for $\rho_{\mathrm{I}}^{1,2}$ and $\rho_{\mathrm{I}}^{\mathrm{e},1}$, $\hat{Z}$ for $\rho_{\mathrm{I}}^{1,1}$, $\rho_{\mathrm{I}}^{1,\mathrm{e}}$ and $\rho_{\mathrm{I}}^{\mathrm{e},2}$, $\hat{X}$ for $\rho_{\mathrm{I}}^{2,4}$ and $\rho_{\mathrm{I}}^{\mathrm{e},3}$, and $\hat{X}\hat{Z}$ for $\rho_{\mathrm{I}}^{2,3}$, $\rho_{\mathrm{I}}^{2,\mathrm{e}}$ and $\rho_{\mathrm{I}}^{\mathrm{e},4}$.

The final teleported state is then

$$\begin{aligned} \rho_{\mathrm{I}}^T(\tau) = &|\mu|^2\big(t^2|+\rangle\langle +| + r^2|0\rangle\langle 0|\big) \otimes |t\alpha\rangle\langle t\alpha| \\ &+ |\nu|^2\big(t^2|-\rangle\langle -| + r^2|0\rangle\langle 0|\big) \otimes |-t\alpha\rangle\langle -t\alpha| \\ &+ t^2 e^{-4|\alpha|^2 r^2}\big(\mu\nu^*|+\rangle\langle -| \otimes |t\alpha\rangle\langle -t\alpha| + \mu^*\nu|-\rangle\langle +| \otimes |-t\alpha\rangle\langle t\alpha|\big), \end{aligned} \tag{37}$$

regardless of the outcomes of the Bell-state measurements. The success probability is

$$\begin{aligned} P_{\mathrm{I}}(\tau) &= \sum_{j=1}^{2} \mathrm{Tr}_{c,C}[\rho^{1,j}] + \sum_{j=3}^{4} \mathrm{Tr}_{c,C}[\rho^{2,j}] + \sum_{i=1}^{2} \mathrm{Tr}_{c,C}[\rho^{i,\mathrm{e}}] + \sum_{j=1}^{4} \mathrm{Tr}_{c,C}[\rho^{\mathrm{e},j}] \\ &= t^2\Big(1 - \frac{1}{2}e^{-2|\alpha|^2 t^2}\Big), \end{aligned} \tag{38}$$

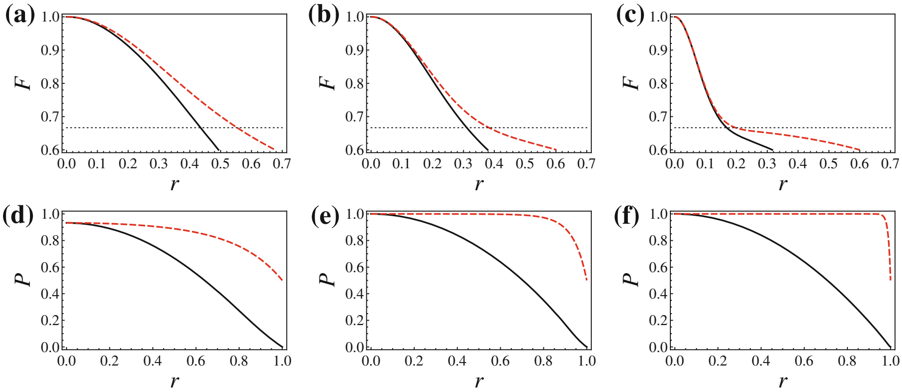

Fig. 2 (Color Online) **a–c** Average fidelities and **d–f** average success probabilities of the type-I hybrid qubits (*black solid curves*) and the type-II hybrid qubits (*red dashed curves*) against the normalized time r. The *horizontal dotted lines* indicate classical limit, 2/3, which can be achieved by using a separable teleportation channel. Graphs are plotted with various values of amplitude α of coherent states as $|\alpha| = 1$ for **a** and **d**, $|\alpha| = 2$ for **b** and **e**, and $|\alpha| = 5$ for **c** and **f**

where the trace was taken over for Bob's part. The average fidelity between the input state $|\phi(\tau)\rangle$ and the teleported state $\rho_{\rm I}^{T}(\tau)$ is

$$F_{\rm I}(\tau) = \frac{1}{4\pi}\int_0^{2\pi}\int_0^{\pi} \langle\phi(\tau)|\rho_{\rm I}^{T}(\tau)|\phi(\tau)\rangle \sin u \mathrm{d}u\mathrm{d}v = \frac{1}{3}t^2(2+e^{-4|\alpha|^2r^2}). \quad (39)$$

The average is taken over in the Bloch sphere of all possible input states $|\phi(\tau)\rangle = \cos(u/2)|0_L(\tau)\rangle + e^{iv}\sin(u/2)|1_L(\tau)\rangle$ to be teleported. The results of the average fidelity and success probability are plotted in Fig. 2.

3.2 Teleportation of type-II hybrid qubits

We consider quantum teleportation of type-II hybrid qubits over a lossy environment. We assume that each mode of the channel state $|\Psi_{ch}\rangle$ suffers the same decoherence rate γ as before. The entangled channel at time τ under above assumption is obtained using Eq. (23) as

$$\begin{aligned}\rho_{\rm II}^{ch}(\tau) = \frac{1}{2}\Big\{&\big[\rho_{++}\otimes|t\alpha\rangle\langle t\alpha|\big]^{\otimes 2} + \big[\rho_{--}\otimes|-t\alpha\rangle\langle -t\alpha|\big]^{\otimes 2}\\ &+\big[e^{-2|\alpha|^2r^2}\rho_{+-}\otimes|t\alpha\rangle\langle -t\alpha|\big]^{\otimes 2} + \big[e^{-2|\alpha|^2r^2}\rho_{-+}\otimes|-t\alpha\rangle\langle t\alpha|\big]^{\otimes 2}\Big\},\end{aligned} \quad (40)$$

where

$$\rho_{++} = \frac{1+t}{2}|+\rangle\langle +| + \frac{1-t}{2}|-\rangle\langle -| + \frac{r^2}{2}|+\rangle\langle -| + \frac{r^2}{2}|-\rangle\langle +|, \quad (41)$$

$$\rho_{--} = \frac{1-t}{2}|+\rangle\langle+| + \frac{1+t}{2}|-\rangle\langle-| + \frac{r^2}{2}|+\rangle\langle-| + \frac{r^2}{2}|-\rangle\langle+|, \tag{42}$$

$$\rho_{+-} = \frac{t^2+t}{2}|+\rangle\langle-| + \frac{t^2-t}{2}|-\rangle\langle+|, \tag{43}$$

$$\rho_{-+} = (\rho_{+-})^\dagger, \tag{44}$$

and $|\pm\rangle = (|0\rangle \pm |1\rangle)/\sqrt{2}$. As before, we use the dynamic qubit basis for coherent states and define the new orthonormal basis as Eq. (27), $|0_L(\tau)\rangle = |+\rangle|t\alpha\rangle$ and $|1_L(\tau)\rangle = |-\rangle|-t\alpha\rangle$, where $|\pm\rangle = (|0\rangle \pm |1\rangle)/\sqrt{2}$, and an unknown hybrid qubit which Alice wants to teleport as $|\phi(\tau)\rangle = \mu|0_L(\tau)\rangle + \nu|1_L(\tau)\rangle$. The logical Bell-state measurement should be performed on the input state $|\phi(\tau)\rangle$ and one part of the decohered channel state $\rho^{ch}_{\text{II}}(\tau)$. The Bell-state measurement for the vacuum and the single-photon states, $\text{B}^{\text{II}}_{\text{s}}$, and that of the coherent states, B_α, are taken. The projection operators of the B_α measurement are already introduced in Sect. 3.1. The $\text{B}^{\text{II}}_{\text{s}}$ measurement is represented by following projection operators,

$$E_1 = |0\rangle_a\langle 0| \otimes |1\rangle_b\langle 1|, \tag{45}$$

$$E_2 = |1\rangle_a\langle 1| \otimes |0\rangle_b\langle 0|, \tag{46}$$

$$E_{\text{e}} = |0\rangle_a\langle 0| \otimes |0\rangle_b\langle 0| + |0\rangle_a\langle 0| \otimes |2\rangle_b\langle 2| + |2\rangle_a\langle 2| \otimes |0\rangle_b\langle 0|, \tag{47}$$

where Ψ^+_{II} and Ψ^-_{II} correspond to E_1 and E_2, and E_{e} represents a measurement failure. The teleportation process will be successful unless both B_α and $\text{B}^{\text{II}}_{\text{s}}$ fail.

The unnormalized state after measurement outcome $E_i \otimes O_j$ is obtained as

$$\rho^{i,j}_{\text{II}} = \text{Tr}_{a,b,A,B}[(U_{a,b} \otimes U_{A,B})(|\phi(\tau)\rangle\langle\phi(\tau)| \otimes \rho^{ch}_{\text{II}}(\tau))(U^\dagger_{a,b} \otimes U^\dagger_{A,B})(E_i \otimes O_j)]. \tag{48}$$

Bob should perform appropriate logical gate operations ($\mathbb{1}$, $\hat{Z}$, $\hat{X}$, or $\hat{X}\hat{Z}$) according to measurement results of Alice. The details are as follows: $\mathbb{1}$ for $\rho^{1,2}_{\text{II}}$, $\rho^{2,1}_{\text{II}}$ and $\rho^{\text{e},1}_{\text{II}}$, $\hat{Z}$ for $\rho^{1,1}_{\text{II}}$, $\rho^{2,2}_{\text{II}}$, $\rho^{\text{e},2}_{\text{II}}$ and $\rho^{1,\text{e}}_{\text{II}}$, $\hat{X}$ for $\rho^{1,3}_{\text{II}}$, $\rho^{2,4}_{\text{II}}$ and $\rho^{\text{e},3}_{\text{II}}$, and $\hat{X}\hat{Z}$ for $\rho^{1,4}_{\text{II}}$, $\rho^{2,3}_{\text{II}}$, $\rho^{\text{e},4}_{\text{II}}$ and $\rho^{2,\text{e}}_{\text{II}}$. As discussed in Sect. 2.2, we assume that when the Pauli Z operation is necessary to complete the teleportation process, we do not apply it directly on the output but rather logically relabel $|0\rangle$ and $|1\rangle$.

The final teleported states after applying appropriate unitary transforms are different from each other according to the Bell-state measurement results. We present all possible teleported states (ρ^T_i), their probabilities (p_i) of obtaining such particular outcomes, and fidelities (f_i) with the input state $|\phi(\tau)\rangle$ in "Appendix." Here we consider the average fidelity and the average success probability as

$$F_{\text{II}}(\tau) = \frac{1}{4\pi}\int_0^{2\pi}\int_0^{\pi} \frac{\sum_i p_i f_i}{\sum_i p_i} \sin u \, du \, dv, \tag{49}$$

$$P_{\text{II}}(\tau) = \frac{1}{4\pi}\int_0^{2\pi}\int_0^{\pi} \sum_i p_i \sin u \, du \, dv, \tag{50}$$

where the average is taken for all possible input states $|\phi(\tau)\rangle$ to be teleported and the summations run over 1 to 5. It is difficult to perform the integration in Eq. (49) in an analytical way because of the summation in the denominator, and we obtain the average fidelity $F_{\mathrm{II}}(\tau)$ numerically using MATHEMATICA. The average success probability in Eq. (50) is obtained as $P_{\mathrm{II}}(\tau) = 1 - \exp(-2|\alpha|^2 t^2)/2$; as one can see, the overall factor of t^2 in Eq. (38) is not here. While a qubit of the vacuum and the single photon in a type-II hybrid qubit after photon loss still remain in the logical qubit space, a polarized single-photon qubit in type-I hybrid qubit evolve out of the logical qubit space due to the addition of the vacuum element under photon loss effects. Such a difference between type-I and type-II qubits makes the drop of the factor t^2.

We plot the average fidelity and the average success probability in Fig. 2. We also compare these results with the results obtained with the type-I qubits in Sect. 3.1. Our results in Fig. 2 clearly show that the average fidelity and the average success probability for type-II are always higher than those of type-I. Again, this can be attributed to the difference in the decoherence mechanism that a qubit of the vacuum and the single photon (type-II) remains in the qubit space under photon loss effects, while a polarized single-photon qubit (type-I) gets out of the qubit space.

4 Remarks

In this paper, we have discussed two types of hybrid qubits for quantum teleportation. One is the hybrid of a polarized single-photon qubit and a coherent-state qubit (type-I), and the other is the hybrid of a qubit of the vacuum and the single-photon and a coherent-state qubit (type-II). Using these two different types of hybrid qubits, we have analyzed the performance of quantum teleportation taking into account both the success probability and output fidelity under the effects of photon losses on the hybrid entangled channels. We found that both the average fidelity and the success probability of teleportation using the type-II hybrid qubits are always higher than those of the type-I hybrid qubits. The reason for this result is that a type-II hybrid qubit always, even under the effects of photon losses, remains in the logical qubit space spanned by the vacuum and the single-photon states. On the other hand, the leakage from the logical qubit space possibly occurs for the type-I hybrid qubits under the photon loss effects, due to the addition of the vacuum element to the photon polarization states. This difference leads to such lower fidelity and success probability for the type-I hybrid qubits. Our results show that the type-II hybrid qubits employing the vacuum and the single-photon states in the single-photon part may be better candidates of hybrid teleportation over a lossy environment. Our result is consistent with the previous study of single-mode qubits [35] where the qubits of the vacuum and the single photon were found to be more efficient than the polarized single-photon qubits for the direct transmission and quantum teleportation.

For future studies, it will be worth investigating the performance of two different types of hybrid qubits in the implementation of scalable quantum computation. For this, there are additional important factors to consider such as error correction models and fault-tolerant limits under the photon losses as well as resource requirements [9]. The effects of photon losses on quantum computation using the type-I hybrid qubit were already studied in Ref. [24]. In a similar way, it may be possible to investigate fault-tolerant limits for the type-II hybrid qubit under the photon loss effects and compare the results with those obtained with type-I qubits. In order to analyze and compare their performance more faithfully, it may be necessary to identify an appropriate error correction model for the type-II hybrid qubits.

Acknowledgments This work was supported by the National Research Foundation of Korea (NRF) grant funded by the Korea government (MSIP) (No. 2010-0018295) and by the KIST Institutional Program (Progect No. 2E26680-16-P025).

Appendix

In this appendix, we present all possible teleported states, their probabilities of obtaining such particular outcomes and fidelities with the input state $|\phi(\tau)\rangle$ for the teleportation of type-II hybrid qubits. All the listed states are the final teleported states on which appropriate unitary transforms are applied. If the measurement results are revealed as $E_1 \otimes O_2$, $E_1 \otimes O_3$, $E_2 \otimes O_1$ and $E_2 \otimes O_4$, the final teleported states are

$$\rho_1^T(\tau) = |\mu|^2 \rho_{++} \otimes |t\alpha\rangle\langle t\alpha| + |\nu|^2 \rho_{--} \otimes |-t\alpha\rangle\langle -t\alpha| \\ + te^{-4|\alpha|^2 r^2} \big(\mu\nu^* \rho_{+-} \otimes |t\alpha\rangle\langle -t\alpha| + \mu^*\nu\rho_{-+} \otimes |-t\alpha\rangle\langle t\alpha|\big), \tag{51}$$

with the probability

$$p_1(\tau) = \mathrm{Tr}_{c,C}[\rho^{1,2}] + \mathrm{Tr}_{c,C}[\rho^{1,3}] + \mathrm{Tr}_{c,C}[\rho^{2,1}] + \mathrm{Tr}_{c,C}[\rho^{2,4}] \\ = \frac{1}{4}\left(1 - e^{-2|\alpha|^2 t^2}\right)\left(1 + te^{-2|\alpha|^2 t^2}\right). \tag{52}$$

Their fidelities with the input state $|\phi(\tau)\rangle$ are calculated as

$$f_1(\tau) = (|\mu|^4 + |\nu|^4)\frac{1+t}{2} + 2|\mu|^2|\nu|^2\left(\frac{1-t}{2}e^{-4|\alpha|^2 t^2} + t\frac{t^2+t}{2}e^{-4|\alpha|^2 r^2}\right) \\ + \left(\mu^2\nu^{*2} + \mu^{*2}\nu^2\right) t\frac{t^2-t}{2}e^{-4|\alpha|^2} + (\mu\nu^* + \mu^*\nu)\frac{r^2}{2}e^{-2|\alpha|^2 t^2}. \tag{53}$$

If the measurement results are revealed as $E_1 \otimes O_1$, $E_1 \otimes O_4$, $E_2 \otimes O_2$ and $E_2 \otimes O_3$, the final teleported states are

$$\rho_2^T(\tau) = |\mu|^2 \rho'_{++} \otimes |t\alpha\rangle\langle t\alpha| + |\nu|^2 \rho'_{--} \otimes |-t\alpha\rangle\langle -t\alpha| \\ + te^{-4|\alpha|^2 r^2} \big(\mu\nu^* \rho_{+-} \otimes |t\alpha\rangle\langle -t\alpha| + \mu^*\nu\rho_{-+} \otimes |-t\alpha\rangle\langle t\alpha|\big), \tag{54}$$

where

$$\rho'_{++} = \frac{1+t}{2}|+\rangle\langle +| + \frac{1-t}{2}|-\rangle\langle -| - \frac{r^2}{2}|+\rangle\langle -| - \frac{r^2}{2}|-\rangle\langle +|, \tag{55}$$

$$\rho'_{--} = \frac{1-t}{2}|+\rangle\langle+| + \frac{1+t}{2}|-\rangle\langle-| - \frac{r^2}{2}|+\rangle\langle-| - \frac{r^2}{2}|-\rangle\langle+|, \tag{56}$$

with the probability

$$\begin{aligned} p_2(\tau) &= \mathrm{Tr}_{c,C}[\rho^{1,1}] + \mathrm{Tr}_{c,C}[\rho^{1,4}] + \mathrm{Tr}_{c,C}[\rho^{2,2}] + \mathrm{Tr}_{c,C}[\rho^{2,3}] \\ &= \frac{1}{4}\left(1 - e^{-2|\alpha|^2 t^2}\right)\left(1 - te^{-2|\alpha|^2 t^2}\right), \end{aligned} \tag{57}$$

and the fidelities are

$$\begin{aligned} f_2(\tau) = {} & (|\mu|^4 + |\nu|^4)\frac{1+t}{2} + 2|\mu|^2|\nu|^2\left(\frac{1-t}{2}e^{-4|\alpha|^2 t^2} + t\frac{t^2+t}{2}e^{-4|\alpha|^2 r^2}\right) \\ & + \left(\mu^2\nu^{*2} + \mu^{*2}\nu^2\right) t\frac{t^2-t}{2}e^{-4|\alpha|^2} - (\mu\nu^* + \mu^*\nu)\frac{r^2}{2}e^{-2|\alpha|^2 t^2}. \end{aligned} \tag{58}$$

If the measurement results are revealed as $E_{\mathrm{e}} \otimes O_1$ and $E_{\mathrm{e}} \otimes O_3$, the final teleported states are

$$\begin{aligned} \rho_3^T(\tau) = {} & |\mu|^2\rho_{++} \otimes |t\alpha\rangle\langle t\alpha| + |\nu|^2\rho_{--} \otimes |-t\alpha\rangle\langle -t\alpha| \\ & + t^2 e^{-4|\alpha|^2 r^2}\left(\mu\nu^*\rho_{+-} \otimes |t\alpha\rangle\langle -t\alpha| + \mu^*\nu\rho_{-+} \otimes |-t\alpha\rangle\langle t\alpha|\right), \end{aligned} \tag{59}$$

with the probability

$$p_3(\tau) = \mathrm{Tr}_{c,C}[\rho^{\mathrm{e},1}] + \mathrm{Tr}_{c,C}[\rho^{\mathrm{e},3}] = \frac{1}{4}\left(1 - e^{-2|\alpha|^2 t^2}\right)^2, \tag{60}$$

and the fidelities are

$$\begin{aligned} f_3(\tau) = {} & (|\mu|^4 + |\nu|^4)\frac{1+t}{2} + 2|\mu|^2|\nu|^2\left(\frac{1-t}{2}e^{-4|\alpha|^2 t^2} + t^2\frac{t^2+t}{2}e^{-4|\alpha|^2 r^2}\right) \\ & + \left(\mu^2\nu^{*2} + \mu^{*2}\nu^2\right) t^2\frac{t^2-t}{2}e^{-4|\alpha|^2} + (\mu\nu^* + \mu^*\nu)\frac{r^2}{2}e^{-2|\alpha|^2 t^2}. \end{aligned} \tag{61}$$

If the measurement results are revealed as $E_{\mathrm{e}} \otimes O_2$ and $E_{\mathrm{e}} \otimes O_4$, the final teleported states are

$$\begin{aligned} \rho_4^T(\tau) = {} & |\mu|^2\rho'_{++} \otimes |t\alpha\rangle\langle t\alpha| + |\nu|^2\rho'_{--} \otimes |-t\alpha\rangle\langle -t\alpha| \\ & + t^2 e^{-4|\alpha|^2 r^2}\left(\mu\nu^*\rho_{+-} \otimes |t\alpha\rangle\langle -t\alpha| + \mu^*\nu\rho_{-+} \otimes |-t\alpha\rangle\langle t\alpha|\right), \end{aligned} \tag{62}$$

with the probability

$$p_4(\tau) = \mathrm{Tr}_{c,C}[\rho^{\mathrm{e},2}] + \mathrm{Tr}_{c,C}[\rho^{\mathrm{e},4}] = \frac{1}{4}(1 - e^{-2|\alpha|^2 t^2})(1 + e^{-2|\alpha|^2 t^2}), \tag{63}$$

and the fidelities are

$$f_4(\tau) = (|\mu|^4 + |\nu|^4)\frac{1+t}{2} + 2|\mu|^2|\nu|^2\left(\frac{1-t}{2}e^{-4|\alpha|^2t^2} + t^2\frac{t^2+t}{2}e^{-4|\alpha|^2r^2}\right)$$
$$+ \left(\mu^2\nu^{*2} + \mu^{*2}\nu^2\right)t^2\frac{t^2-t}{2}e^{-4|\alpha|^2} - (\mu\nu^* + \mu^*\nu)\frac{r^2}{2}e^{-2|\alpha|^2t^2}. \quad (64)$$

Lastly, for the measurement results of $E_1 \otimes O_\mathrm{e}$ and $E_2 \otimes O_\mathrm{e}$, the final teleported states are

$$\rho_5^T(\tau) = \frac{1}{1-(\mu\nu^* + \mu^*\nu)r^2}$$
$$\times \left\{\left(|\mu|^2\frac{1+t}{2} - \mu\nu^*\frac{r^2}{2} - \mu^*\nu\frac{r^2}{2} + |\nu|^2\frac{1-t}{2}\right)\rho'_{++} \otimes |t\alpha\rangle\langle t\alpha|\right.$$
$$+ \left(|\mu|^2\frac{1-t}{2} - \mu\nu^*\frac{r^2}{2} - \mu^*\nu\frac{r^2}{2} + |\nu|^2\frac{1+t}{2}\right)\rho'_{--} \otimes |-t\alpha\rangle\langle -t\alpha|$$
$$+ e^{-4|\alpha|^2r^2}\left[\left(\mu\nu^*\frac{t^2+t}{2} + \mu^*\nu\frac{t^2-t}{2}\right)\rho_{+-} \otimes |t\alpha\rangle\langle -t\alpha|\right.$$
$$\left.\left. + \left(\mu\nu^*\frac{t^2-t}{2} + \mu^*\nu\frac{t^2+t}{2}\right)\rho_{-+} \otimes |-t\alpha\rangle\langle t\alpha|\right]\right\} \quad (65)$$

with the probability

$$p_5(\tau) = \mathrm{Tr}_{c,C}[\rho^{1,\mathrm{e}}] + \mathrm{Tr}_{c,C}[\rho^{2,\mathrm{e}}] = \frac{1}{2}e^{-2|\alpha|^2t^2}\left[1-(\mu\nu^* + \mu^*\nu)r^2\right], \quad (66)$$

and the fidelities are

$$f_5(\tau) = \frac{1}{1-(\mu\nu^* + \mu^*\nu)r^2}\left\{(|\mu|^4 + |\nu|^4)\left[\left(\frac{1+t}{2}\right)^2 + \left(\frac{1-t}{2}\right)^2 e^{-4|\alpha|^2t^2}\right]\right.$$
$$+ 2|\mu|^2|\nu|^2\left[\frac{r^2}{4}\left(1+e^{-2|\alpha|^2t^2}\right)^2 + \left(\frac{t^2+t}{2}\right)^2 e^{-4|\alpha|^2r^2} + \left(\frac{t^2-t}{2}\right)^2 e^{-4|\alpha|^2}\right]$$
$$+ (\mu^2\nu^{*2} + \mu^{*2}\nu^2)\left[\frac{r^4}{2}e^{-2|\alpha|^2t^2} + \left(\frac{t^2+t}{2}\right)\left(\frac{t^2-t}{2}\right)\left(e^{-4|\alpha|^2r^2} + e^{-4|\alpha|^2}\right)\right]$$
$$\left. - (\mu\nu^* + \mu^*\nu)\frac{r^2}{2}\left(1+e^{-2|\alpha|^2t^2}\right)\left(\frac{1+t}{2} + \frac{1-t}{2}e^{-2|\alpha|^2t^2}\right)\right\}. \quad (67)$$

References

1. Bennett, C.H., Brassard, G., Crépeau, C., Jozsa, R., Peres, A., Wootters, W.K.: Teleporting an unknown quantum state via dual classical and Einstein–Podolsky–Rosen channels. Phys. Rev. Lett. **70**, 1895–1899 (1993)
2. Bouwmeester, D., Pan, J.-W., Mattle, K., Eibl, M., Weinfurter, H., Zeilinger, A.: Experimental quantum teleportation. Nature (London) **390**, 575–579 (1997)

3. Pirandola, S., Eisert, J., Weedbrook, C., Furusawa, A., Braunstein, S.L.: Advances in quantum teleportation. Nat. Photonics **9**, 641–652 (2015)
4. Gottesman, D., Chuang, I.L.: Demonstrating the viability of universal quantum computation using teleportation and single-qubit operations. Nature (London) **402**, 390–393 (1999)
5. Knill, E., Laflamme, R., Milburn, G.J.: A scheme for efficient quantum computation with linear optics. Nature (London) **409**, 46–52 (2001)
6. Dawson, C.M., Haselgrove, H.L., Nielsen, M.A.: Noise thresholds for optical cluster-state quantum computation. Phys. Rev. A **73**, 052306 (2006)
7. Hayes, A.J.F., Haselgrove, H.L., Gilchrist, A., Ralph, T.C.: Fault tolerance in parity-state linear optical quantum computing. Phys. Rev. A **82**, 022323 (2010)
8. Lund, A.P., Ralph, T.C., Haselgrove, H.L.: Fault-tolerant linear optical quantum computing with small-amplitude coherent states. Phys. Rev. Lett. **100**, 030503 (2008)
9. Ralph, T.C., Pryde, G.J.: Optical quantum computation. Prog. Opt. **54**, 209–269 (2010)
10. Lee, H.-W., Kim, J.: Quantum teleportation and Bell's inequality using single-particle entanglement. Phys. Rev. A **63**, 012305 (2000)
11. Lund, A.P., Ralph, T.C.: Nondeterministic gates for photonic single-rail quantum logic. Phys. Rev. A **66**, 032307 (2002)
12. Lütkenhaus, N., Calsamiglia, J., Suominen, K.-A.: Bell measurements for teleportation. Phys. Rev. A **59**, 3295–3300 (1999)
13. Calsamiglia, J., Lütkenhaus, N.: Maximum efficiency of a linear-optical Bell-state analyzer. Appl. Phys. B **72**, 67–71 (2001)
14. Grice, W.P.: Arbitrarily complete Bell-state measurement using only linear optical elements. Phys. Rev. A **84**, 042331 (2011)
15. Zaidi, H.A., van Loock, P.: Beating the one-half limit of ancilla-free linear optics Bell measurements. Phys. Rev. Lett. **110**, 260501 (2013)
16. Ewert, F., van Loock, P.: 3/4-efficient Bell measurement with passive linear optics and unentangled ancillae. Phys. Rev. Lett. **113**, 140403 (2014)
17. Lee, S.-W., Park, K., Ralph, T.C., Jeong, H.: Nearly deterministic Bell measurement for multiphoton qubits and its application to quantum information processing. Phys. Rev. Lett. **114**, 113603 (2015)
18. Lee, S.-W., Park, K., Ralph, T.C., Jeong, H.: Nearly deterministic Bell measurement with multiphoton entanglement for efficient quantum-information processing. Phys. Rev. A **92**, 052324 (2015)
19. van Enk, S.J., Hirota, O.: Entangled coherent states: teleportation and decoherence. Phys. Rev. A **64**, 022313 (2001)
20. Jeong, H., Kim, M.S., Lee, J.: Quantum-information processing for a coherent superposition state via a mixed entangled coherent channel. Phys. Rev. A **64**, 052308 (2001)
21. Jeong, H., Kim, M.S.: Efficient quantum computation using coherent states. Phys. Rev. A **65**, 042305 (2002)
22. Jeong, H., Kim, M.S.: Purification of entangled coherent states. Quantum Inf. Comput. **2**, 208–221 (2002)
23. Ralph, T.C., Gilchrist, A., Milburn, G.J., Munro, W.J., Glancy, S.: Quantum computation with optical coherent states. Phys. Rev. A **68**, 042319 (2003)
24. Lee, S.-W., Jeong, H.: Near-deterministic quantum teleportation and resource-efficient quantum computation using linear optics and hybrid qubits. Phys. Rev. A **87**, 022326 (2013)
25. Park, K., Lee, S.-W., Jeong, H.: Quantum teleportation between particlelike and fieldlike qubits using hybrid entanglement under decoherence effects. Phys. Rev. A **86**, 062301 (2012)
26. Kwon, H., Jeong, H.: Violation of the Bell–Clauser–Horne–Shimony–Holt inequality using imperfect photodetectors with optical hybrid states. Phys. Rev. A **88**, 052127 (2013)
27. Gerry, C.C.: Generation of optical macroscopic quantum superposition states via state reduction with a Mach–Zehnder interferometer containing a Kerr medium. Phys. Rev. A **59**, 4095–4098 (1999)
28. Jeong, H.: Using weak nonlinearity under decoherence for macroscopic entanglement generation and quantum computation. Phys. Rev. A **72**, 034305 (2005)
29. Munro, W.J., Nemoto, K., Spiller, T.P.: Weak nonlinearities: a new route to optical quantum computation. New J. Phys. **7**, 137 (2005)
30. Shapiro, J.H., Razavi, M.: Continuous-time cross-phase modulation and quantum computation. New J. Phys. **9**, 16 (2007)
31. Kwon, H., Jeong, H.: Generation of hybrid entanglement between a single-photon polarization qubit and a coherent state. Phys. Rev. A **91**, 012340 (2015)

32. Ourjoumtsev, A., Jeong, H., Tualle-Brouri, R., Grangier, P.: Generation of optical 'Schrödinger cats' from photon number states. Nature (London) **448**, 784–786 (2007)
33. Jeong, H., Zavatta, A., Kang, M., Lee, S.-W., Costanzo, L.S., Grandi, S., Ralph, T.C., Bellini, M.: Generation of hybrid entanglement of light. Nat. Photonics **8**, 564–569 (2014)
34. Morin, O., Huang, K., Liu, J., Jeannic, H.L., Fabre, C., Laurat, J.: Remote creation of hybrid entanglement between particle-like and wave-like optical qubits. Nat. Photonics **8**, 570–574 (2014)
35. Kim, H., Park, J., Jeong, H.: Transfer of different types of optical qubits over a lossy environment. Phys. Rev. A **89**, 042303 (2014)
36. Walls, D.F., Milburn, G.J.: Effect of dissipation on quantum coherence. Phys. Rev. A **31**, 2403–2408 (1985)
37. Oh, S., Lee, S., Lee, H.-W.: Fidelity of quantum teleportation through noisy channels. Phys. Rev. A **66**, 022316 (2002)
38. Man, Z.-X., Xia, Y.-J.: Quantum teleportation in a dissipative environment. Quantum Inf. Process. **11**, 1911–1920 (2012)
39. De Martini, F.: Amplification of quantum entanglement. Phys. Rev. Lett. **81**, 2842–2845 (1998)
40. De Martini, F., Sciarrino, F., Vitelli, C.: Entanglement test on a microscopic–macroscopic system. Phys. Rev. Lett. **100**, 253601 (2008)
41. Sekatski, P., Sanguinetti, B., Pomarico, E., Gisin, N., Simon, C.: Cloning entangled photons to scales one can see. Phys. Rev. A **82**, 053814 (2010)
42. Sekatski, P., Sangouard, N., Stobińska, M., Bussières, F., Afzelius, M., Gisin, N.: Proposal for exploring macroscopic entanglement with a single photon and coherent states. Phys. Rev. A **86**, 060301(R) (2012)
43. Ghobadi, R., Lvovsky, A., Simon, C.: Creating and detecting micro–macro photon-number entanglement by amplifying and deamplifying a single-photon entangled state. Phys. Rev. Lett. **110**, 170406 (2013)
44. Bruno, N., Martin, A., Sekatski, P., Sangouard, N., Thew, R.T., Gisin, N.: Displacement of entanglement back and forth between the micro and macro domains. Nat. Phys. **9**, 545–548 (2013)
45. Lvovsky, A.I., Ghobadi, R., Chandra, A., Prasad, A.S., Simon, C.: Observation of micromacro entanglement of light. Nat. Phys. **9**, 541–544 (2013)
46. Andersen, U.L., Neergaard-Nielsen, J.S.: Heralded generation of a micro–macro entangled state. Phys. Rev. A **88**, 022337 (2013)
47. Sheng, Y.-B., Zhou, L., Long, G.-L.: Hybrid entanglement purification for quantum repeaters. Phys. Rev. A **88**, 022302 (2013)
48. Takeda, S., Mizuta, T., Fuwa, M., van Loock, P., Furusawa, A.: Deterministic quantum teleportation of photonic quantum bits by a hybrid technique. Nature (London) **500**, 315–318 (2013)
49. Andersen, U.L., Neergaard-Nielsen, J.S., van Loock, P., Furusawa, A.: Hybrid discrete- and continuous-variable quantum information. Nat. Phys. **11**, 713–719 (2015)
50. Louisell, W.H.: Quantum Statistical Properties of Radiation. Wiley, New York (1973)
51. Phoenix, S.J.D.: Wave-packet evolution in the damped oscillator. Phys. Rev. A **41**, 5132–5138 (1990)